Surface Science Letters 285 (1993) L461–L467
North-Holland

surface science letters

Surface Science Letters

Mixtures of Kr and Xe physisorbed on Pt(111): a prototype of a stochastic two-dimensional alloy

Peter Zeppenfeld [a], Klaus Kern [b], Rudolf David [a], Ulrich Becher [a] and George Comsa [a]

[a] *Institut für Grenzflächenforschung und Vakuumphysik, KFA Forschungszentrum Jülich, Postfach 1913, 5170 Jülich, Germany*
[b] *Institut de Physique Expérimentale, EPF Lausanne, PHB-Ecublens, CH-1015 Lausanne, Switzerland*

Received 15 December 1992; accepted for publication 7 January 1993

Krypton and xenon co-adsorbed on the Pt(111) surface at 40 K are found to form homogenous stochastic mixtures for all composition ratios and in the entire coverage regime below one monolayer. These quasi two-dimensional $Kr_{1-\chi}Xe_{\chi}$ alloys ($0 \leq \chi \leq 1$) are characterized by narrow diffraction peaks indicating a high degree of positional as well as orientational order. The position of the diffraction peaks of the mixture varies linearly as a function of the molar fraction χ between those of the pure Kr and Xe components (Vegard's law). The half-widths of the diffraction peaks are larger than for the pure Kr system but even at $\chi = 0.5$ quasi crystalline order still extends over a length scale of about 100 Å. The diffraction line-shapes are well described within a simple model of lattice disorder.

Recently, disordered systems have attracted great interest among surface scientists. The increased performance and sensitivity of the experimental techniques together with the development of powerful theoretical tools and computational methods make it possible to investigate increasingly complex systems and to study perturbations of ordered systems due to impurities, steps, or disorder. All naturally occurring surfaces will exhibit *some* type of disorder, such as thermal vibrations and structural defects. It was realized very early, that disorder plays an important role in many of the physical and chemical properties of surfaces. Sticking, chemical reactivity, or crystal growth may even be governed entirely by impurity atoms or steps present on the surface. It was also noticed that the disordering at surfaces can involve new phases and processes which are not encountered in three-dimensional crystals. For instance, the melting transition which is known to be of first order in bulk crystals was shown to be a continuous transition at the crystal surface [1]. Similarly, the quasi two-dimensional phase of an adsorbate layer or thin film can melt in two successive steps [2]: first the quasi crystalline phase will loose its positional order but still retain its long range orientational correlation. In the case of a hexagonal close packed system this phase is called the "hexatic" liquid. It has no analogue in three dimensions. In a second transition the hexatic phase then disorders to form a classic liquid with only short range positional and orientational order. In the experiment, the existence of a hexatic phase, however, is still disputed [3].

Here we want to present another class of quasi two-dimensional disordered systems, namely the binary mixtures of sub-monolayer amounts of rare gas species adsorbed on a single-crystal surface. The disorder which is introduced by mixing two different rare gas species originates from the size mismatch of the two rare gas atoms which will impair the formation of long-range ordered (crystalline) structures. The interesting feature of this type of disorder is that the mismatch can be simply set by choosing the appropriate combinations of differently sized atoms, and that the disorder can be further controlled by varying the mixing ratio. This, together with the fact that the interactions among the rare gases are well known

and that reliable rare-gas/metal potentials are becoming available, make the two-dimensional rare gas mixtures candidates for model systems in the study of disorder in two dimensions. By comparing the properties of the two-dimensional mixtures with those of bulk alloys we also hope to gain insight into the effect of the reduced dimensionality and into the role of the substrate on the mixing. There have been several studied on binary two-dimensional mixtures which have dealt mainly with the identification of ordered stochiometry phases and the corresponding phase diagram [4] as well as with the effect of intermixing on structural phase transitions [5].

We have used He scattering to study the structure of the rare gas mixtures Ar–Kr, Kr–Xe, and Ar–Xe adsorbed on the Pt(111) surface. Here we present our results on the Kr–Xe system which has a moderate structural mismatch, characterized by an atomic diameter ratio $a_{Kr}/a_{Xe} = 0.916$ at 40 K. This system is found to form a complete, stochastic mixture of the two components with a high degree of quasi-crystalline order in the resulting two-dimensional alloy. The results for the other two binary mixtures focusing on the thermodynamics and kinetics of the mixing (Ar–Kr) and the ordering in the case of large atomic size mismatch (Ar–Xe) will be presented elsewhere [6].

The experimental set-up used in the experiments is described in detail in ref. [7]. We briefly summarize its main characteristics: The supersonic He beam is generated by expanding He gas from a pressure of about 150 bar through a small nozzle (5 μm in diameter). The resulting He beam is highly monochromatic ($\Delta E/E = 1.4\%$). It is directed at the sample and the scattered He atoms are detected in a quadrupole mass spectrometer. The total scattering angle is fixed ($\vartheta_i + \vartheta_f = 90°$) and the scattering conditions are varied by rotating the sample about an axis normal to the scattering plane yielding a parallel momentum transfer $Q = k_i[\sin(\vartheta_i) - \sin(\vartheta_f) = \sqrt{2}k_i \sin(\vartheta_i - 45°)$. The azimuthal orientation of the sample can be varied by rotating the crystal about its surface normal leaving the polar angle and wave vector transfer unchanged. The angular divergence of the incident beam and the angle subtended by the detector are both 0.2°. Together with the energy spread of the incident beam this results in a wave vector resolution of the apparatus of about 0.01 A^{-1}. The sample temperature can be varied from 25 to 1500 K. The Pt(111) sample is a high quality surface with an average terrace width ≥ 2000 Å [8]. It was cleaned by cycles of Ar sputtering and heating in oxygen until no traces of impurities could be detected by Auger spectroscopy. Before each experiment the sample was cleaned by sputtering with Ar and subsequent annealing at about 1000 K. The sample smoothness and cleanliness was routinely checked by monitoring the He reflectivity, which constitutes a sensitive probe for defects and impurities [9].

The rare gases were adsorbed onto the Pt(111) substrate by exposing the sample to a partial pressure of the rare gas. The amount actually adsorbed on the surface (i.e., the coverage) can be accurately determined by monitoring the decrease of the He reflectivity as a function of exposure [10]. Once this coverage calibration is established the desired rare gas coverage can be controlled within an estimated error of $\pm 5\%$ by dosing the appropriate amount. In the present case the two components Kr and Xe were adsorbed successively, first Kr followed by Xe. By monitoring the He reflectivity, it was checked that the presence of Kr does not modify (within the accuracy of our experiment) the adsorption properties of the Xe as compared to the adsorption on the clean Pt(111) surface: on the clean as well as on the Kr pre-covered Pt(111) surface the sticking probability for Xe is close to unity. In the following we will only discuss our results on mixtures in the sub-monolayer coverage regime, i.e., in which the platinum surface is not completely covered with Kr and Xe. In fact, close to monolayer completion both the Xe and Kr adlayer undergo structural phase transitions [11,12] that obscure the properties of the Kr–Xe mixture which are of primary interest here. Besides the total coverage the most important parameter used for the characterization of the mixture is the relative composition. In the following we will use the molar fraction χ defined as the ratio between the number of Xe atoms and the total number of

SURFACE SCIENCE LETTERS

Kr and Xe atoms on the surface to quantify the composition of the mixture. Thus:

$$\chi_{Xe} \equiv \frac{N_{Xe}}{N_{Kr} + N_{Xe}}. \quad (1)$$

We will omit the subscript "Xe" in the following to refer to the xenon molar fraction. The Kr molar fraction is simply given by $\chi_{Kr} = 1 - \chi$. The molar fraction is easily deduced from the partial Kr and Xe coverages.

Once the two components are adsorbed on the surface the structure is investigated by taking polar and azimuthal diffraction scans yielding the size and orientation of the unit cell. If the rare gases are adsorbed at low surface temperature (≤ 25 K) separate Kr and Xe nth order diffraction peaks are observed along the $\overline{\Gamma K}$-azimuth of the Pt(111) substrate indicating the formation of two distinct hexagonal phases rotated by 30° with respect to the underlying substrate. The wave vector positions of the diffraction peaks are close to the positions found in the pure Kr and Xe phases which demonstrates that at these low temperatures Kr and Xe are still phase separated after successive adsorption. After annealing the system at about 35 K, however, only single nth order diffraction peaks along the $\overline{\Gamma K}$-azimuth are observed whose positions are located between those for the pure phases. As will be demonstrated later this single "intermediate" diffraction peak is characteristic for the *complete stochastically* mixed Kr–Xe phase. The same diffraction signature is obtained if Kr and Xe are adsorbed at elevated temperature (above 35 K) and if Kr and Xe are dosed simultaneously instead of being adsorbed successively. The thermodynamics and kinetics of the mixing will not be discussed in greater detail here. For this the reader is referred to a forthcoming paper [6]. All the experimental results presented here was obtained from complete mixtures that were carefully annealed at about 40 K.

Fig. 1 shows a series of polar diffraction scans around the position of the second order diffraction peak (2,0) of the mixture (which happens to be more intense than the corresponding first order diffraction peak). The top panel depicts the scan for the pure Kr component adsorbed at 40 K. The lower panels show diffraction scans after co-adsorption of Xe at 40 K. It is obvious that the position of the diffraction peak shifts from its initial position at $8\pi/(\sqrt{3}\, a_{Kr}) = 3.52$ Å^{-1} (corresponding to a Kr nearest neighbour distance of $a_{Kr} = 4.12$ Å) towards smaller wave vector Q as the xenon molar fraction χ increases. The position of the (2,0) peak of the pure Xe incommensurate phase on Pt(111) would be 3.22 Å^{-1} ($a_{Xe} = 4.50$ Å). It is evident from fig. 1 that the position of the diffraction peak of the mixture

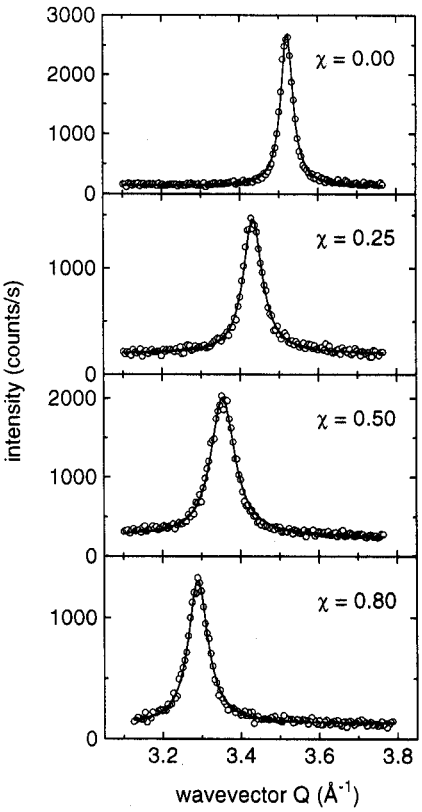

Fig. 1. He-diffraction scans around the (2,0) Bragg-peak for a Kr–Xe binary mixture adsorbed on a Pt(111) substrate at $T = 40$ K for various composition ratios (given by the Xe molar fraction χ). The corresponding total coverages (defined here as the total number of Kr and Xe atoms N per cm^2) from top to bottom panel are 1.66×10^{14}, 2.21×10^{14}, 3.31×10^{14} and 0.80×10^{14} cm^{-2}. The single diffraction peak and its continuous shift with χ is a signature of the homogeneous, stochastic nature of the mixture. The solid lines through the data points are fits to eq. (4).

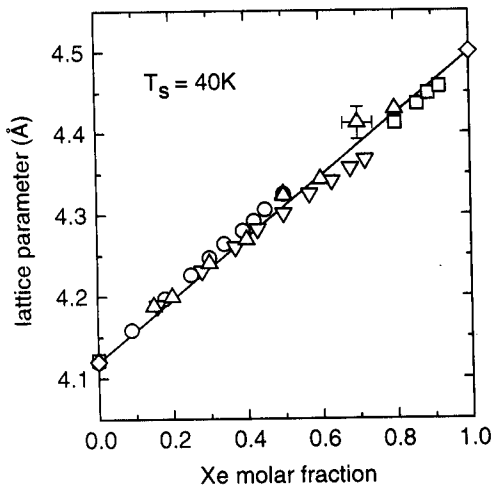

Fig. 2. Average lattice parameter of the Kr–Xe mixture as obtained from the He-diffraction peak position as a function of Xe molar fraction. Symbols ○, ▽ and □ correspond to experimental runs with a Kr pre-coverage of 1.66×10^{14}, 0.83×10^{14} and 0.17×10^{14} cm^{-2}, respectively (and thus different total coverage for the same χ). The data points △ were all taken at about the same *total* coverage of $(3.4\pm0.3)\times10^{14}$ cm^{-2}. The solid line corresponds to the linear interpolation between the lattice parameter of the pure components with χ according to Vegard's law.

varies monotonically with χ. At the same time, the diffraction peak width increases only slightly and even the mixture at $\chi = 0.5$ exhibits a relatively narrow diffraction peak (much narrower than the amount by which the peak is shifted away from the position of the diffraction peaks of the pure components). Therefore, the diffraction peak of the mixed phase can be viewed as originating from a well ordered phase consisting of atoms of an "average" size. A quantitative evaluation of this average nearest neighbour distance as obtained from the position of the diffraction peaks of a large number of scans is presented in fig. 2. The different symbols represent different experiments, each starting with a different initial Kr coverage and successively adding Xe. Thus, different symbols at the same value of χ also correspond to different *total* coverages. The nearest neighbour distance in the mixed phase varies in a continuous, linear fashion as a function of molar fraction between the nearest neighbour distances of the pure Kr and Xe components:

$$a = \chi a_{Xe} + (1-\chi)a_{Kr}. \qquad (2)$$

This relationship is known as "Vegard's law" and was first observed for three-dimensional binary allows [13]. A similar variation of a in adsorbate systems was also observed for Kr–Xe mixtures on graphite [14]. In a one-dimensional mixture of atoms of type A and B Vegard's law can be understood in terms of the statistic mean of the separation between neighbouring particles arranged along a chain in a random distribution, where χ and $(1-\chi)$ are the probability of the particle being an A or B atom, respectively. Unlike an *independent* random displacement around a mean position as for instance in the case of a crystal at finite temperature, the pair correlation function (i.e., the probability of finding a particle at a distance $r = na$ from any reference atom) is not constant but decreases with $r \to \infty$. The reason for this is the fact that the position of atom number n depends on the type of all the atoms between the reference point and the nth atom. If the arrangement is purely stochastic and if the atoms are assumed to behave like hard spheres with diameters a_A and a_B, respectively, the $n+1$ possible positions of atom number n will be $r(n, k) = na_A + k(a_B - a_A)$, $k = 0 \cdots n$, with a probability according to a polynomial distribution $p[r(n, k)] = \chi^k(1-\chi)^{n-k}$. Hence, the mean distance is given by $r(n, k) = na$ with $a = \chi_A + (1-\chi)a_B$ according to eq. (2), while the variance around this mean position is $\sigma^2(n) = n(a_B - a_A)^2\chi(1-\chi)$, increasing linearly with separation n. As a consequence, the order in this stochastic mixture model will not be of long range, even though for small size mismatch of atoms A and B relatively sharp diffraction peaks can still be obtained. This is easily shown by calculating the diffraction pattern from such a stochastic one-dimensional mixture, given by the square of the Fourier-transform of the position correlation function $\sum_{n=0}^{\infty}\sum_{k=1}^{n} p[r(n, k)]$. This problem can be solved numerically, but there also exists an analytical solution for the limit of $p[r(n, k)]$ becoming a continuous Gaussian distribution

$g[r(n)]$ with the same values for the mean and standard deviation na and $\sigma(n)$, respectively [15]:

$$g[r(n)] = \frac{1}{\sqrt{2\pi n\sigma^2}} e^{-(r-na)^2/2n\sigma^2},$$

$$\text{with } \sigma^2 = \chi(1-\chi)(a_B - a_A)^2. \quad (3)$$

For the diffraction intensity $I(Q)$, with Q being the momentum transfer, one obtains:

$$I(Q) = I_0 \frac{1-\alpha^2}{1+\alpha^2-2\alpha\cos(Qa)}, \quad (4a)$$

$$\text{where } \alpha = \exp\left(-\tfrac{1}{2}Q^2\sigma^2\right). \quad (4b)$$

Eq. (4a) describes a series of diffraction peaks at positions $Q^{(m)} = 2\pi m/a$ (with m being an integer) whose FWHM is given by

$$\Delta Q^{(m)} = \frac{2}{a}\cos^{-1}\left(\frac{4\alpha - \alpha^2 - 1}{2\alpha}\right). \quad (5)$$

For small σ, $\Delta Q^{(m)}$ increases proportionally to m^2. In the tails of the diffraction peaks described by eq. (4) the diffracted intensity decays algebraically as $I(Q) \sim Q^{-2}$. Eq. (4) is very similar to the formula obtained in ref. [16] for the case of randomly distributed terraces on a surface with the important difference that in ref. [16] α is a constant. The *increase* of the FWHM with the order of the diffraction peak in the present case is a signature of the imperfect crystallinity of the structure of the stochastic mixture.

We will now discuss our experimental results and compare them to the simple model of lattice disorder described above. As already mentioned and evidenced in fig. 2, Vegard's law (eq. 2) is obeyed over the entire range of molar fraction χ and total coverage. This means that there are no regions in the composition phase diagram for surface temperatures around 40 K in which Kr–Xe binary mixtures would phase separate or form stochiometrically stable mixtures. Instead, Kr and Xe form *homogenous stochastic* mixtures. Furthermore, the line-shape given by eq. (4) fit the experimental diffraction spectra quite well. This is demonstrated in fig. 1 which shows experimental spectra together with the best fit to eq. (4) treating α and I_0 as independent fitting parameters. Fig. 3 shows the results of the fitting of a

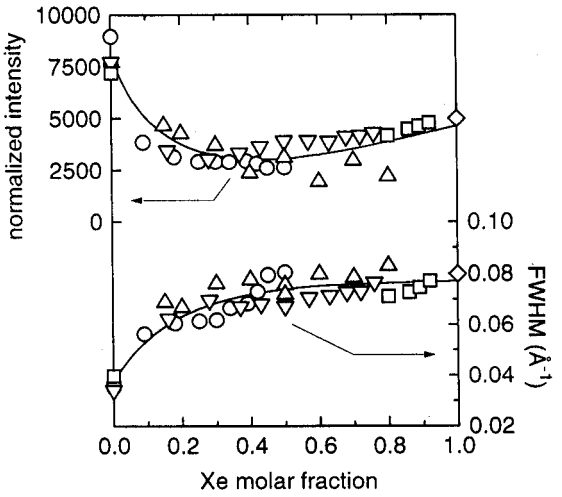

Fig. 3. Fitting of the experimental diffraction line-shapes for the (2,0) Bragg-peak as illustrated in fig. 1: Peak intensities normalized to the total coverage (top panel) and peak widths (FWHM) (lower panel) as a function of the Xe molar fraction; symbols as in fig. 2.

large number of diffraction spectra. In the upper panel the fitted intensity of the diffraction peak, divided by the total coverage for normalization, is plotted. Being largest for the pure components the intensity decreases with increasing admixture of the minority component leading to a minimum at around $\chi = 0.5$. This can be easily understood since for $\chi = 0.5$ the mixture is expected to be most disordered. The lower panel of fig. 3 shows the dependency of the FWHM on the Xe molar fraction. From eq. (4b) with $\sigma^2 = \chi(1-\chi)(a_{Xe} - a_{Kr})^2$ we would expect a quadratic variation of the FWHM of the diffraction peaks as a function of χ which should be symmetric around $\chi = 0.5$. This is not observed in fig. 3, because of the way the instrumental broadening adds to the theoretical line-width: the pure xenon phase forms a rather badly ordered incommensurate phase at 40 K [11]. This is reflected in the FWHM of about 0.08 $Å^{-1}$ of the second order diffraction peak for the pure Xe phase as compared to 0.034 $Å^{-1}$ for the pure Kr phase. Hence, the broadening due to the admixture of xenon can be safely evaluated only in the Kr-rich regime. In the range from $\chi = 0$ to 0.20 the total FWHM increases from 0.034 to 0.064 $Å^{-1}$, which corresponds to an

effective broadening of $\Delta Q^{(2)} = 0.054$ Å^{-1} assuming that the widths add Gaussian. Similarly, we found the increase of the FWHM for the first order diffraction peak $\Delta Q^{(1)}$ to be only about 0.028 Å^{-1}. This has to be compared to the values derived from the one-dimensional model $\Delta Q^{(1)} = 0.012$ Å^{-1} and $\Delta Q^{(2)} = 0.046$ Å^{-1}, respectively. Hence, the experimental values show that the peak broadening is of the right order of magnitude and that it is, indeed, larger for the second order diffraction peak than for the first order peak. This demonstrates a certain loss of crystalline order. However, the relatively smaller increase of the experimental peak-width as compared to the factor of 4 predicted from eq. (5) indicates a rather good accommodation of the lattice mismatch. This becomes even more evident from the evaluation of eq. (5), and eq. (4b) at $\chi = 0.5$ yielding $\Delta Q^{(2)} = 0.082$ Å^{-1}, which is much larger than the maximum residual peak width observed experimentally.

Although the comparison with a one-dimensional model leads to a fairly good agreement with the experimental data, it is important to realize that our system is a *two-dimensional* one. One might therefore expect a smaller degree of ordering as well as a possible orientational disorder due to an imperfect two-dimensional packing of the atoms within the adlayer. Unfortunately, there are no simple analytic theories (as the one described above) for the case of a two-dimensional stochastic mixture. There exists a number of experiments, which have investigated the properties of binary mixtures of differently sized macroscopic discs [17], and computer simulation on these non-interacting systems [18]. As an important result these simulations generate stochastic mixtures which are orientationally ordered and display quasi-crystalline positional order for all composition ratios if the discs size-difference does not exceed 10–15%. This result is related to the empirical Hume–Rothery rule formulated for the case of bulk alloys [19]. Only recently a Monte-Carlo simulation for the Kr–Xe system on the Pt(111) surface has been performed [20] and the results are in excellent agreement with our experimental data: Indeed, Gerber et al. find that Kr and Xe form a homogeneous, almost perfectly stochastic mixture at 40 K; the mean lattice parameter follows Vegard's law and the positional order is quasi-crystalline. Furthermore, they find that the orientational order is undisturbed and the symmetry directions of the adlayer structure are aligned with the Pt(111) substrate. Due to this alignment, it is not clear whether the perfect orientational order is an intrinsic property of the mixture or whether it is stabilized by the substrate. An interesting result obtained in ref. [20], which might explain the rather small perturbation of the cristallinity observed both in experiment and simulation, is the fact that the Kr and Xe atoms do not sit at the same distance from the Pt surface: There is a difference of approximately 0.25 Å in the distances. According to Gerber et al. "this slight 'bilayer-like' structure plays a role in reducing packing strains, and stabilizing the periodic structure despite the different sizes of the two constituent atoms" [20b].

The authors gratefully acknowledge stimulating discussions with R.B. Gerber.

References

[1] J.W.M. Frenken and J.F. van der Veen, Phys. Rev. Lett. 54 (1985) 134;
J.F. van der Veen, B. Pluis and A.W. Denier van der Gon, in: Chemistry and Physics of Solid Surfaces VII, Vol. 10 of Springer Series in Surface Science (Springer, Berlin, 1988) 455.

[2] J.M. Kosterlitz and D.J. Thouless, J. Phys. C 6 (1973) 1181;
D.R. Nelson and B.L. Halperin, Phys. Rev. B 19 (1979) 2457;
A.P. Young, Phys. Rev. B 19 (1979) 1855;
W. Janke and H. Kleinhert, Phys. Rev. Lett. 61 (1988) 2344.

[3] R.J. Birgeneau and P.M. Horn, Science 232 (1986) 329;
A.J. Jin, M.R. Bjurstrom and M.H.W. Chan, Phys. Rev. Lett. 62 (1988) 1372.

[4] H. You and S.C. Fain, Phys. Rev. B 34 (1986) 2840;
N.K. Mahale and M.W. Cole, Surf. Sci. 176 (1986) 319;
A. Razafitanamaharavo, P. Convert, B. Croset and N. Dupont-Pavlovsky, J. Phys. (Paris) 51 (1990) 1961.

[5] J. Bohr, M. Nielsen, J. Als-Nielsen, K. Kjaer and J.P. McTague, Surf. Sci. 125 (1983) 181;
J.W. Stephens, A.I. Goldman, P.A. Heiney and P.A. Bancel, Phys. Rev. B 33 (1986) 655.

[6] P. Zeppenfeld, U. Becher, K. Kern, R. David and G. Comsa, to be published.

[7] R. David, K. Kern, P. Zeppenfeld and G. Comsa, Rev. Sci. Instrum. 57 (1986) 2771.
[8] B. Poelsema, R.L. Palmer, G. Mechtersheimer and G. Comsa, Surf. Sci. 117 (1982) 60.
[9] B. Poelsema and G. Comsa, Scattering of Thermal Energy Atoms from Disordered Surfaces, Vol. 115 of Springer Tracts in Modern Physics (Springer, Berlin, 1989).
[10] K. Kern and G. Comsa, in: Kinetics of Ordering and Growth at Surfaces, Ed. M.G. Lagally (Plenum, New York, 1990) 53.
[11] K. Kern, R. David, P. Zeppenfeld, R.L. Palmer and G. Comsa, Solid State Commun. 62 (1987) 391.
[12] K. Kern, P. Zeppenfeld, R. David and G. Comsa, Phys. Rev. Lett. 59 (1987) 79.
[13] L. Vegard and H. Dale, Z. Kristallogr. 67 (1928) 148.
[14] T. Ceva, M. Goldmann and C. Marti, J. Phys. (Paris) 47 (1986) 1527.
[15] J.M. Cowley, Diffraction Physics (North-Holland, Amsterdam, 1990) 152.
[16] P. Fenter and T.-M. Lu, Surf. Sci. 154 (1985) 15;
J.M. Pimbley and T.-M. Lu, J. Appl. Phys. 57 (1985) 1121.
[17] A.S. Nowick and S.R. Mader, IBM J. Res. Dev. Sept.–Nov. (1965) 348.
[18] D.R. Nelson, M. Rubinstein and F. Saepen, Philos. Mag. A 46 (1982) 105;
M. Rubinstein and D.R. Nelson, Phys. Rev. B 26 (1982) 6254.
[19] W. Hume-Rothery, R.E. Smallman and C.W. Harworth, The Structure of Metals and Alloys (The Metals and Metallurgy Trust, London, 1969);
J.L. Barrat, M. Baus and J.P. Hansen, Phys. Rev. Lett. 56 (1986) 1063.
[20] R.B. Gerber and A.T. Yinnon, Chem. Phys. Lett. 181 (1991) 553;
R.B. Gerber, A.T. Yinnon, M. Yanuka and D. Chase, Surf. Sci. 272 (1992) 81.